

We have made similar calculations for the lateral spread of high energy nucleons in lead and find, for example, that under a block of 56-cm thickness the root-mean-square distance from the shower axis of particles with energy above 10 Bev is 6.4 cm. Owing to the constant density of the medium, the maximum spread is not attained within several meters of lead.

It is hoped to present a more detailed account of this work shortly.

<sup>1</sup> G. Molière, *Cosmic Radiation*, edited by W. Heisenberg (Dover Publications, New York, 1946).

<sup>2</sup> J. Roberg and L. W. Nordheim, *Phys. Rev.* **75**, 444 (1949).

<sup>3</sup> A. Borsellino, *Nuovo cimento* **7**, 4 (1950).

<sup>4</sup> H. S. Green and H. Messel, *Phys. Rev.* **83**, 842 (1951); *Proc. Phys. Soc. (London)* (to be published).

<sup>5</sup> H. Messel and H. S. Green, *Phys. Rev.* **83**, 1279 (1951).

<sup>6</sup> D. V. Skobeltsyn *et al.*, *Dokl. Akad. Nauk. S.S.S.R.* **73**, 1157 (1950).

<sup>7</sup> G. T. Zatspein *et al.*, *Dokl. Akad. Nauk. S.S.S.R.* **74**, 29 (1950).

<sup>8</sup> L. K. Eidus *et al.*, *Dokl. Akad. Nauk. S.S.S.R.* **75**, 669 (1950).

## The Drift Mobility of Electrons in Silicon

J. R. HAYNES AND W. C. WESTPHAL  
Bell Telephone Laboratories, Murray Hill, New Jersey  
(Received December 26, 1951)

THE mobility of electrons injected into *p*-type silicon has been determined by measuring transit times between the emitter and collector points with single crystal rods.

The techniques used to measure the drift mobility of injected carriers in germanium<sup>1</sup> were altered in these measurements not only because the shape of the advancing wave front of injected carriers in silicon is affected by a temporary trapping but also because of the much higher impedance of voltage probe points.

A schematic diagram of the circuit used successfully with silicon is shown in Fig. 1. Electrons are injected at the time of the current pulse and flow down the crystal under the influence of the electric field. When the pulse of electrons arrives at the collector point, a signal is produced.<sup>2</sup> A sketch of the oscilloscope pattern obtained is shown in Fig. 2. The dots represent 10- $\mu$ sec marker intervals. The current pulse used to inject the electrons produces a corresponding voltage pulse at the start of the oscilloscope trace as a result of the resistance of the silicon rod between the collector point and ground. After this initial pulse the voltage remains constant for some 40 microseconds. During this time the injected electrons are moving down the silicon crystal from the emitter point which was placed a centimeter away from the collector. When the electron pulse arrives at the collector, the voltage pulse shown is observed. The transit time,  $t$ , for the injected electrons is the time represented by the distance from the center of the voltage pulse to the maximum signal produced by the arrival of the electron pulse.

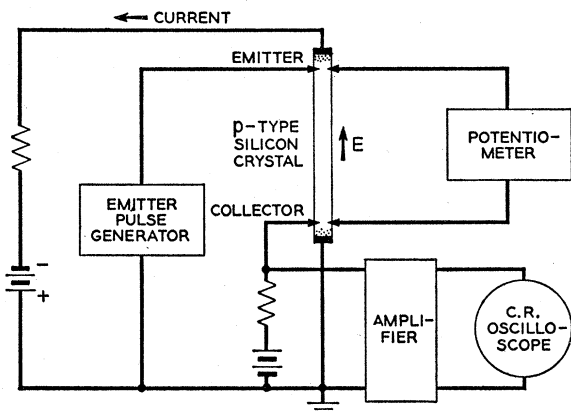


FIG. 1. Schematic of circuit used to measure the drift mobility of injected electrons in silicon.

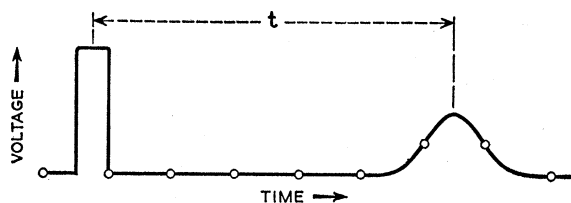


FIG. 2. Drawing of oscilloscope trace showing time of injection pulse and subsequent electron arrival.

It is found that the transit time measured in this way is a function of the amplitude of the current pulse as a result of conductivity modulation of the silicon rod. As the amplitude of the current pulse is continuously decreased, the signal arrival time becomes earlier, at first rapidly and then more slowly. The transit time corrected for conductivity modulation could therefore easily be obtained visually by extrapolating the locus of arrival time points to zero signal.

The drift mobility  $\mu_D$  of electrons in silicon was calculated from the relation  $\mu_D = L^2/Vt$ , where  $t$  is the transit time,  $L$  is the distance from emitter to collector, and  $V$  is the voltage difference in silicon between emitter and collector.

Representative values of  $L$  and  $V$  used are shown in Table I together with the resultant measured transit time. The corresponding value of  $\mu_D$  has been corrected for nonuniformity of electric field and temperature rise produced by the dc current.<sup>1</sup> The average value of mobility obtained for all data is 1210  $\text{cm}^2/\text{volt sec}$ .

TABLE I. Representative values of electron drift mobility data.

Sample No.	$L$ (cm)	$V$ (volts)	$t$ ( $\mu$ sec)	$\mu_D$ ( $\text{cm}^2/\text{volt sec}$ )
I	0.537	5.70	43.9	1204
I	1.10	12.3	84.0	1248
I	1.12	29.5	41.8	1194
II	0.64	5.56	63.3	1190
II	0.64	11.8	32.6	1162
II	0.64	4.49	73.8	1283

This value is more than four times as large as the mobility of electrons in silicon reported by Pearson and Bardeen<sup>3</sup> (300  $\text{cm}^2/\text{volt sec}$  for electrons, 100  $\text{cm}^2/\text{volt sec}$  for holes). Their values, however, were obtained from Hall effect data in multicrystalline samples, and their extremely low values were most probably caused by inhomogeneities produced by crystal grain boundaries.

In view of the experience with germanium, it is felt that even though only two samples have been examined, the drift mobility of electrons in silicon is within 10 percent of 1200  $\text{cm}^2/\text{volt sec}$ . Preliminary measurements with injected holes in *n*-type silicon indicate a drift mobility for holes in the neighborhood of 250  $\text{cm}^2/\text{volt sec}$  giving a ratio of electron to hole mobility of 4.8.

The authors are indebted to W. Shockley for advice and to G. K. Teal and E. Buehler who provided the silicon ingot.

<sup>1</sup> J. R. Haynes and W. Shockley, *Phys. Rev.* **81**, 835 (1951).

<sup>2</sup> See reference 1 for a more complete description of the main features of the circuit.

<sup>3</sup> G. L. Pearson and J. Bardeen, *Phys. Rev.* **75**, 865 (1949).

## Photomeson Production in Carbon and Hydrogen\*

B. T. FELD, D. H. FRISCH, I. L. LEBOW, L. S. OSBORNE, AND J. S. CLARK  
Physics Department and Laboratory for Nuclear Science and  
Engineering, Massachusetts Institute of Technology,  
Cambridge 39, Massachusetts  
(Received January 4, 1952)

CYLINDRICAL targets of paraffin, heavy paraffin, and graphite were exposed simultaneously to the x-ray spectrum produced by 330-Mev electrons in the M.I.T. synchrotron. The

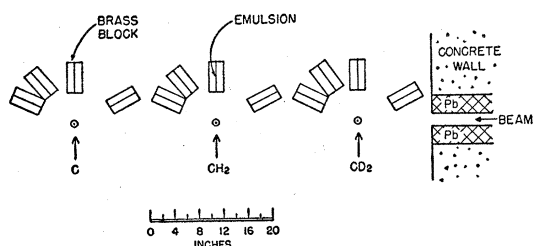


FIG. 1. Schematic diagram of the experiment for the observation of the spectra of photomesons from hydrogen, deuterium, and carbon.

energy distributions of photomesons from carbon and hydrogen have been obtained at angles of  $90^\circ$  and  $26^\circ$  to the photon beam. The mesons were slowed down in  $2\frac{1}{2}$ -in. wide  $\times$  4-in. high  $\times$  5-in. long brass blocks, and the ends of their tracks were observed in 200- $\mu$  unbacked Ilford C-3 photographic emulsions embedded radially in blocks, as shown in Fig. 1. The location of each meson track ending was recorded as a function of its depth in the block.

Positive  $\pi$ -mesons are identified by their  $\mu$ -decay. Negative  $\pi$ -mesons are identified as those which produce nuclear disintegrations (stars), plus a predetermined fraction of those mesons ending without any visible disintegration products.<sup>1</sup> The distribution of mesons in energy is obtained by dividing the emulsions into intervals of equal meson energy, assuming the meson energy to be given by the range in brass corresponding to the distance from the face of the block to the meson ending. (A slight correction of  $\sim 10$  Mev is applied for the thickness of the target.) The hydrogen distributions were obtained by subtracting the carbon distributions from those of the paraffin.

The number of positive mesons per proton in carbon as compared to hydrogen, averaged over the above energy ranges, is  $0.32 \pm 0.05$  (standard deviation) at  $90^\circ$  and  $0.07 \pm 0.01$  at  $26^\circ$ . This large decrease in production efficiency for carbon at forward angles is qualitatively as expected on the basis of the Pauli exclusion principle, since the recoil momentum of the product neutron is small when the meson is emitted forward. Due to the smallness of the carbon production at small angles, the subtraction procedure, to obtain the H cross section, introduces only small uncertainties at  $26^\circ$ .

The negative-positive ratio from carbon shows no strong dependence on meson energy and has the average value of  $1.43 \pm 0.13$

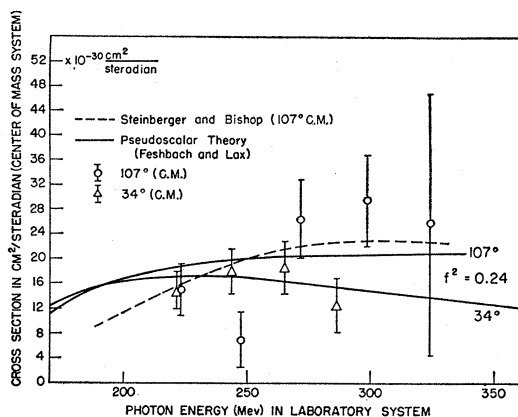


FIG. 2. Comparison of experiment with theory for the differential cross section for photomeson production in hydrogen vs photon energy, for mesons emitted at  $34^\circ$  and  $107^\circ$  in the C.M. system. The experimental points have been corrected for nuclear interactions in the brass moderator. The broken curve summarizes the results of Steinberger and Bishop (see reference 8) at  $107^\circ$ . Our cross sections agree within the factor of two in uncertainty about our absolute intensity at the time of exposure. The points as plotted here are normalized to the experimental curve of Steinberger and Bishop. The solid curves are computed from the theory of Feshbach and Lax (see reference 7), for a (pseudoscalar meson with pseudovector-) coupling constant  $f^2 = 0.24$ .

at  $90^\circ$  and  $1.03 \pm 0.25$  at  $26^\circ$ . Peterson, Gilbert, and White<sup>3</sup> found a value of  $1.30 \pm 0.12$  at  $90^\circ$ . The energy spectra at  $90^\circ$  are in good agreement with previous experiments<sup>3,4</sup> and with theory.<sup>5</sup>

From energy and momentum conservation and assuming a photon spectrum,<sup>6</sup> the hydrogen distributions are converted into cross sections in the center-of-mass system. In Fig. 2, we plot the experimental cross sections vs photon energy for hydrogen together with the predictions of pseudoscalar theory,<sup>7</sup> the Berkeley data<sup>8</sup> at  $107^\circ$ , and our data at  $107^\circ$ . Averaging our cross sections over the approximate range  $h\nu = 210$  to  $h\nu = 305$  Mev, we find  $\bar{\sigma}(34^\circ)/\bar{\sigma}(107^\circ) = 0.80 \pm 0.18$ . This result is not strictly comparable with the observed<sup>3</sup>  $h\nu = 250$  Mev angular distribution, but together they indicate that the average cross section over this energy range does not drop off extremely rapidly at small angles.<sup>9</sup>

We wish to thank Meses. T. Kallmes, D. Calhoun, and M. Goode who performed most of the arduous work of scanning the plates.

\* This work was supported in part by the joint program of the ONR and AEC.

<sup>1</sup> Our determination of the fraction of negative  $\pi$ -mesons which give rise to zero-pronged (neutron) stars is  $35 \pm 4$  percent in a total of 585 stars, which agrees well with the  $32.6 \pm 2.1$  percent found by W. B. Cheston and L. J. B. Goldfarb, Phys. Rev. **78**, 683 (1950).

<sup>2</sup> Bernardini, Booth, and Lederman, Phys. Rev. **83**, 1075 (1951).

<sup>3</sup> Peterson, Gilbert, and White, Phys. Rev. **81**, 1003 (1951).

<sup>4</sup> J. Steinberger and A. S. Bishop, Phys. Rev. **78**, 494 (1950).

<sup>5</sup> M. Lax and H. Feshbach, Phys. Rev. **81**, 189 (1951).

<sup>6</sup> Powell, Hartsough, and Hill, Phys. Rev. **81**, 213 (1951).

<sup>7</sup> H. Feshbach and M. Lax, Phys. Rev. **76**, 134 (1949).

<sup>8</sup> Bishop, Steinberger, and Cook, Phys. Rev. **80**, 291 (1950); J. Steinberger and A. S. Bishop, private communication. Their value for the ratio of cross sections at  $58^\circ$  to  $107^\circ$  ( $45^\circ$  and  $90^\circ$  in the laboratory system) for 250-Mev photons is 0.70 (assuming the correction for nuclear absorption suggested by reference 2).

<sup>9</sup> K. A. Brueckner, Phys. Rev. **79**, 641 (1950).

### Photomeson Production from Deuterium\*

I. L. LEBOW, B. T. FELD, D. H. FRISCH, AND L. S. OSBORNE

Physics Department and Laboratory for Nuclear Science and Engineering, Massachusetts Institute of Technology, Cambridge 39, Massachusetts

(Received January 4, 1952)

WE have measured the energy distributions of the positive and negative  $\pi$ -mesons from deuterium at  $90^\circ$  and  $26^\circ$  to the photon beam. A heavy paraffin target was exposed to the 330-Mev bremsstrahlung spectrum from the M.I.T. synchrotron simultaneously with the exposures of carbon and paraffin targets described in the preceding communication. The methods of detection and analysis of data are also as previously described. The observations are displayed in Figs. 1(a) and 1(b).

Special interest is attached to the investigation of photomeson production from deuterium, mainly for two reasons: (1) The deuteron is the simplest nucleus that can be used to study the production of mesons from neutrons since the ratio of negative to positive production gives a comparison of production from neutrons and protons. We find experimentally that the average  $\pi^-/\pi^+$  yield ratio from the deuteron is  $0.5 \pm 0.5$  at  $90^\circ$  and  $0.90 \pm 0.23$  at  $26^\circ$ . Our present statistics and uncertain knowledge of the absorption in brass do not permit us to conclude that the apparent decrease of the negative to positive ratio with increasing meson energy and angle is real. White<sup>1</sup> has found a ratio of  $0.96 \pm 0.10$  over the spectrum at  $45^\circ$  and a value of  $0.98 \pm 0.14$  for the ratio at  $90^\circ$  for 70-Mev mesons. Littauer and Walker<sup>2</sup> obtained a ratio of  $1.19 \pm 0.12$  for 50-Mev mesons at  $135^\circ$ .

(2) The photoproduction of a charged meson from a deuteron results in a pair of identical nucleons, whose possible quantum states are limited by the Pauli exclusion principle. Since the initial deuteron state is predominantly  $^3S_1$ , the possibility of leaving the final two-nucleon system in an  $S$ -state depends on the occurrence of "spin-flip" in the charged photomeson production reaction. Thus, there should be a greater reduction of  $\pi^+$  production in deuterium, relative to hydrogen, for a spin-independent interaction than for a spin-dependent interaction. This is a marked effect